PHYSICAL REVIEW A **77**, 061603(R) (2008)

Phase-space deformation of a trapped dipolar Fermi gas

Takahiko Miyakawa,[1] Takaaki Sogo,[2,*] and Han Pu[3]
[1]*Department of Physics, Faculty of Science, Tokyo University of Science, 1-3 Kagurazaka, Shinjuku, Tokyo 162-8601, Japan*
[2]*Department of Physics, Kyoto University, Kitashirakawa, Sakyo, Kyoto 606-8502, Japan*
[3]*Department of Physics and Astronomy, and Rice Quantum Institute, Rice University, Houston, Texas 77251, USA*
(Received 27 October 2007; revised manuscript received 2 May 2008; published 9 June 2008)

We consider a system of quantum degenerate spin-polarized fermions in a harmonic trap at zero temperature, interacting via dipole-dipole forces. We introduce a variational Wigner function to describe the deformation and compression of the Fermi gas in phase space and use it to examine the stability of the system. We emphasize the important roles played by the Fock exchange term of the dipolar interaction, which results in a nonspherical Fermi surface.

DOI: 10.1103/PhysRevA.77.061603 PACS number(s): 03.75.Ss, 05.30.Fk, 34.20.−b, 75.80.+q

Two-body collisions in usual ultracold atomic systems can be described by short-range interactions. The successful realization of chromium Bose-Einstein condensates (BECs) [1] and recent progress in creating heteronuclear polar molecules [2] have stimulated great interest in quantum degenerate dipolar gases. The anisotropic and long-range nature of the dipolar interaction makes the dipolar systems different from nondipolar ones in many qualitative ways [3]. Although most of the theoretical studies of dipolar gases have focused on dipolar BECs, where the stability and excitations of the system are investigated (see Ref. [3] and references therein, and also Ref. [4]) and new quantum phases are predicted [5,6], some interesting works about dipolar Fermi gas do exist. These studies concern the ground-state properties [7–9], dipolar-induced superfluidity [10], and strongly correlated states in rotating dipolar Fermi gases [11]. We notice, however, that previous mean-field studies did not consider the dipolar interaction induced Fermi-surface anisotropies such as those discussed in this work.

In this Rapid Communication, we study a system of dipolar spin-polarized Fermi gas. We will show that the Fock exchange term causes the deformation of the Fermi surface as a consequence of the anisotropy of the dipolar interaction. Since the Fermi surface is the determining factor in low-energy properties of the Fermi system, its deformation plays a crucial role in the properties of the dipolar Fermi gas. We will show some important features due to the deformed Fermi surface. Of particular importance is the instability of the dipolar gas. It is also shown that the deformed Fermi surface, which can be readily imaged by time-of-flight technique [12], yields a straightforward way of detecting dipolar effects in Fermi gases. The expansion technique has also been used to detect the dipolar effects in chromium BEC. In that case, the expansion dynamics depends strongly on the initial trap geometry [13,14].

In our work, we consider a trapped dipolar gas of single-component fermions of mass m and magnetic or electric dipole moment $\boldsymbol{d}$ at zero temperature. The dipoles are assumed to be polarized along the z axis. The system is described by the Hamiltonian

$$H=\sum_{i=1}^{N}\left[-\frac{\hbar^2}{2m}\nabla_i^2+U(\boldsymbol{r}_i)\right]+\frac{1}{2}\sum_{i\neq j}V_{dd}(\boldsymbol{r}_i-\boldsymbol{r}_j), \tag{1}$$

where $V_{dd}(\boldsymbol{r})=(d^2/r^3)(1-3z^2/r^2)$ is the two-body dipolar interaction and $U(\boldsymbol{r})$ is the trap potential. In the expression of V_{dd}, the contact term of the dipolar interaction has been neglected because of Fermi statistics [7].

To characterize the system, we use a semiclassical approach in which the one-body density matrix is given by

$$\rho(\boldsymbol{r},\boldsymbol{r}')=\int\frac{d^3k}{(2\pi)^3}f\left(\frac{\boldsymbol{r}+\boldsymbol{r}'}{2},\boldsymbol{k}\right)e^{i\boldsymbol{k}(\boldsymbol{r}-\boldsymbol{r}')}, \tag{2}$$

where $f(\boldsymbol{r},\boldsymbol{k})$ is the Wigner distribution function. The density distributions in momentum and real space are then given, respectively, by $\bar{n}(\boldsymbol{k})=(2\pi)^{-3}\int d^3r f(\boldsymbol{r},\boldsymbol{k})$ and $n(\boldsymbol{r})=\rho(\boldsymbol{r},\boldsymbol{r})=(2\pi)^{-3}\int d^3k f(\boldsymbol{r},\boldsymbol{k})$.

Our goal is to examine $n(\boldsymbol{r})$ and $\bar{n}(\boldsymbol{k})$, as well as the stability of the system, by minimizing the energy functional using a variational method. Within the Thomas-Fermi-Dirac approximation [7], the total energy of the system is given by $E=E_{\mathrm{kin}}+E_{\mathrm{tr}}+E_d+E_{\mathrm{ex}}$, where

$$E_{\mathrm{kin}}=\int d^3r\int\frac{d^3k}{(2\pi)^3}\frac{\hbar^2\boldsymbol{k}^2}{2m}f(\boldsymbol{r},\boldsymbol{k}), \tag{3}$$

$$E_{\mathrm{tr}}=\int d^3rU(\boldsymbol{r})n(\boldsymbol{r}), \tag{4}$$

$$E_d=\frac{1}{2}\int d^3r\int d^3r'V_{dd}(\boldsymbol{r}-\boldsymbol{r}')n(\boldsymbol{r})n(\boldsymbol{r}'), \tag{5}$$

$$E_{\mathrm{ex}}=-\frac{1}{2}\int d^3r\int d^3r'\int\frac{d^3k}{(2\pi)^3}\int\frac{d^3k'}{(2\pi)^3}V_{dd}(\boldsymbol{r}-\boldsymbol{r}')\times e^{i(\boldsymbol{k}-\boldsymbol{k}')\cdot(\boldsymbol{r}-\boldsymbol{r}')}f\left(\frac{\boldsymbol{r}+\boldsymbol{r}'}{2},\boldsymbol{k}\right)f\left(\frac{\boldsymbol{r}+\boldsymbol{r}'}{2},\boldsymbol{k}'\right). \tag{6}$$

The dipolar interaction induces two contributions: the Hartree direct energy E_d and the Fock exchange energy E_{ex}. The latter arises due to the requirement of the antisymmetrization of many-body fermion wave functions and is therefore absent for the dipolar BECs. It is also easy to see that, if V_{dd} in

*Present address: Institut für Physik, Universität Rostock, D-18051 Rostock, Germany.

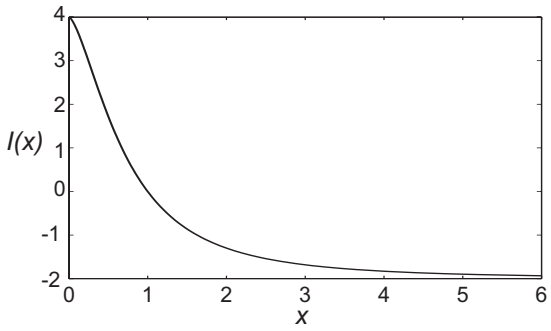

FIG. 1. Deformation function $I(x)$.

Eqs. (5) and (6) are replaced by a contact interaction $\propto\delta(\boldsymbol{r}-\boldsymbol{r}')$, then $E_d=-E_{\rm ex}$, which leads to a total cancellation of the interaction energy. This further justifies the neglect of the contact term in the dipolar potential.

Homogeneous case. Let us first consider a homogeneous system of volume $\mathcal{V}$ with number density n_f, which will provide some insights into the trapped system to be discussed later. We choose a variational ansatz for the Wigner distribution function that is spatially invariant,

$$f(\boldsymbol{r},\boldsymbol{k}) = f(\boldsymbol{k}) = \Theta[k_F^2 - \alpha^{-1}(k_x^2 + k_y^2) - \alpha^2 k_z^2], \tag{7}$$

where $\Theta(\,)$ is Heaviside's step function. Here the positive parameter α represents deformation of the Fermi surface [15]; the constant k_F is the Fermi wave number and is related to the number density through $n_f=k_F^3/6\pi^2$. The choice of Eq. (7) preserves the number density, i.e., $(2\pi)^{-3}\int d^3k f(\boldsymbol{k})=n_f$, and is motivated by the anisotropic nature of the dipolar interaction.

We note that the Hartree direct energy of Eq. (5) becomes zero for uniform density distribution of fermions because the average over an angle in the relative coordinate $\boldsymbol{r}-\boldsymbol{r}'$ cancels out the interaction effect. To evaluate the Fock exchange energy of Eq. (6), we have used the Fourier transform of the dipolar potential $\bar{V}_{dd}(\boldsymbol{q})=(4\pi/3)d^2(3\cos^2\theta_{\boldsymbol{q}}-1)$, where $\theta_{\boldsymbol{q}}$ is the angle between the momentum $\boldsymbol{q}$ and the dipolar direction (i.e., the z axis). Using the variation ansatz (7), the exchange energy can be evaluated analytically and is given by

$$E_{\rm ex} = -\pi d^2 \mathcal{V} I(\alpha) n_f^2/3, \tag{8}$$

where we have defined the "deformation function,"

$$I(x) = \int_0^\pi d\theta \sin\theta \left(\frac{3\cos^2\theta}{x^3\sin^2\theta + \cos^2\theta} - 1 \right).$$

This integral has a rather complicated analytical form. It is more instructive to plot out the function $I(x)$, which we show in Fig. 1. $I(x)$ is a monotonically decreasing function of x, positive for $x<1$, passing through zero at $x=1$, and becomes negative for $x>1$. The exchange energy (8), therefore, tends to stretch the Fermi surface along the z axis by taking $\alpha\to 0$. This, however, comes at the expense of the kinetic energy,

$$E_{\rm kin} = \frac{\mathcal{V}}{5}\frac{\hbar^2 k_F^2}{2m} n_f \left(\frac{1}{\alpha^2} + 2\alpha \right),$$

which favors a spherical Fermi surface (i.e., $\alpha=1$). The competition between the two will find an optimal value of α in the region $\alpha\in(0,1)$. The dipolar interaction, therefore, through the Fock exchange energy, deforms the Fermi surface of the system. This may be regarded as the magnetostriction effect in momentum space.

Inhomogeneous case. Let us now turn to a system of N atoms confined in a harmonic trapping potential with axial symmetry: $U(\boldsymbol{r})=m[\omega_r^2(x^2+y^2)+\omega_z^2 z^2]/2$. We choose a variational Wigner function that has the same form as in the homogeneous case, i.e., Eq. (7), but now the Fermi wave number k_F is no longer a constant and has the following spatial dependence:

$$k_F^2(\boldsymbol{r}) = (\bar{k}_F^{\lambda})^2 - \lambda^2 a_{ho}^{-4}[\beta(x^2+y^2) + \beta^{-2}z^2], \tag{9}$$

where $a_{ho}=\sqrt{\hbar/m\omega}$ and $\omega=(\omega_r^2\omega_z)^{1/3}$. The variational parameters β and λ represent deformation and compression of the dipolar gas in real space, respectively. The ansatz Eq. (9) is motivated by the local-density approximation, which is justified for large number of fermions [15]. Using $N=\int d^3 r n(\boldsymbol{r})$, one can easily find that $\bar{k}_F^{\lambda}=(48N)^{1/6}\lambda^{1/2}/a_{ho}$. The corresponding density distributions in real and momentum space are given by

$$n(\boldsymbol{r}) = \frac{(\bar{k}_F^{\lambda})^3}{6\pi^2}\left\{ 1 - \frac{1}{(R_F^{\lambda})^2}\left[\beta(x^2+y^2) + \frac{1}{\beta^2}z^2 \right] \right\}^{3/2},$$

$$\bar{n}(\boldsymbol{k}) = \frac{(R_F^{\lambda})^3}{6\pi^2}\left\{ 1 - \frac{1}{(\bar{k}_F^{\lambda})^2}\left[\frac{1}{\alpha}(k_x^2+k_y^2) + \alpha^2 k_z^2 \right] \right\}^{3/2},$$

respectively, where $R_F^{\lambda}=(48N)^{1/6}a_{ho}/\lambda^{1/2}$.

Under this ansatz, each term in the energy functional can be evaluated analytically, with the total energy given by, in units of $N^{4/3}\hbar\omega$,

$$\epsilon(\alpha,\beta,\lambda) = c_1\left[\lambda\left(2\alpha + \frac{1}{\alpha^2} \right) + \frac{1}{\lambda}\left(2\frac{\beta_0}{\beta} + \frac{\beta^2}{\beta_0^2} \right) \right] + c_2 c_{dd} N^{1/6}\lambda^{3/2}\{I(\beta) - I(\alpha)\}, \tag{10}$$

where $c_1=3^{1/3}/2^{8/3}\simeq 0.2271$, $c_2=2^{10}/(3^{7/2}\cdot 5\cdot 7\pi^2)\simeq 0.0634$, $c_{dd}=d^2/(a_{ho}^3\hbar\omega)$, and $\beta_0\equiv(\omega_r/\omega_z)^{2/3}$ measures the trap aspect ratio. Here the two terms in the square brackets on the right-hand side represent the kinetic and trapping energy, respectively, while those in the curly brackets are the direct and exchange interaction terms, respectively.

It can be seen that Eq. (10) is not bounded from below, a result arising from the fact that the dipolar interaction is partially attractive. There exists, however, under certain conditions, a local minimum in Eq. (10) representing a metastable state, a situation reminiscent of the case of a trapped attractive BEC [16]. Hereafter, we refer to the metastable state as the ground state.

We find the ground state by numerically minimizing Eq. (10). Figure 2 shows the ground-state density distributions in both real and momentum spaces for two different traps. One

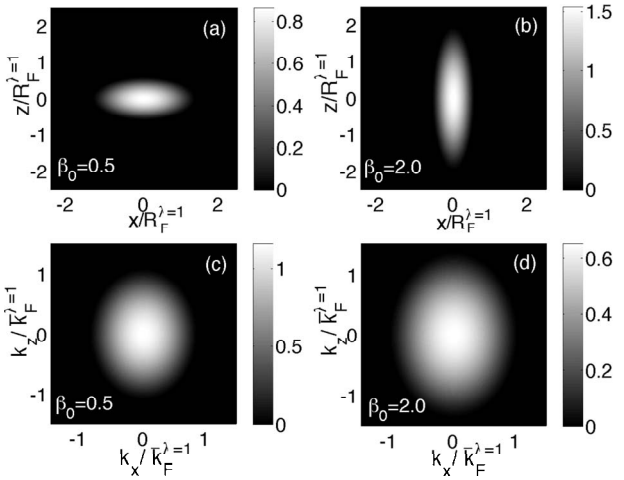

FIG. 2. Density distributions in real space [upper plots, in units of $(\bar{k}_F^{\lambda=1})^3/6\pi^2$] and in momentum space [lower plots, in units of $(R_F^{\lambda=1})^3/6\pi^2$] for an oblate trap with $\beta_0=0.5$ (left plots) and a prolate trap with $\beta_0=2$ (right plots) for $c_{dd}N^{1/6}=1.5$.

can see that while the spatial density distributions are essentially determined by the trap geometry, the momentum density distributions by contrast are quite insensitive to the trapping potential and are in both cases elongated along the dipolar direction.

The stretch in k_z is more clearly illustrated in Fig. 3(a), where we have plotted the ratio of the root-mean-square momentum in the k_z direction, $\sqrt{\langle k_z^2\rangle_0}$, and to that in the k_x direction, $\sqrt{\langle k_x^2\rangle_0}$, as a function of the trap aspect ratio β_0 for several dipolar strengths. It turns out that the dipolar interaction leads to nonspherical momentum distribution stretched along the dipolar direction irrespective of the geometry of the trapping potential. This can be attributed to the Fock exchange energy that becomes negative for $\alpha<1$ as discussed in the homogeneous system. This result is in stark contrast to the case of dipolar BECs in which the Fock exchange energy is absent and the shape of the momentum distribution is related to that of the spatial distribution through the Fourier transformation [17]. Note that, for noninteracting fermions, the resulting momentum distribution is isotropic independent of the trapping potential [18,19].

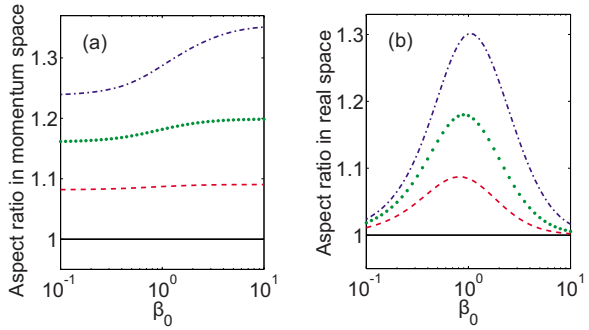

FIG. 3. (Color online) (a) Aspect ratio in momentum space $\sqrt{\langle k_z^2\rangle_0/\langle k_x^2\rangle_0}$ and (b) aspect ratio in real space $\sqrt{\langle z^2\rangle_0/\langle x^2\rangle_0}$ normalized to that for a noninteracting system as functions of β_0 for $c_{dd}N^{1/6}=0$ (solid line), 0.5 (dashed line), 1 (dotted line), and 1.5 (dot-dashed line).

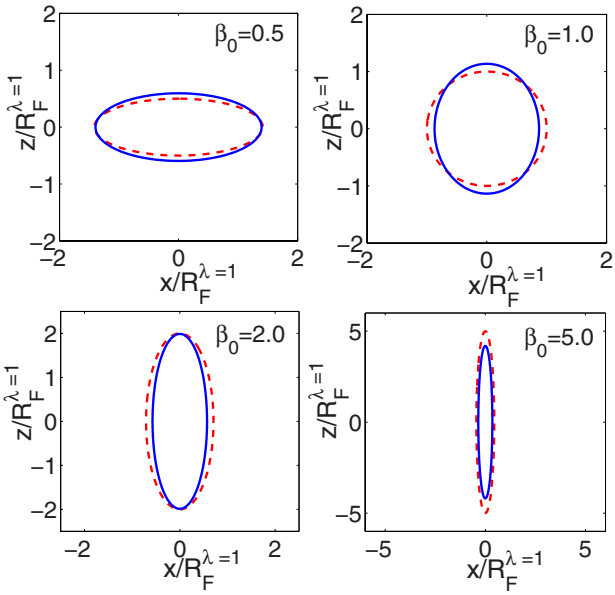

FIG. 4. (Color online) Thomas-Fermi surface in real space of the ground state for the noninteracting case (dashed line) and for interacting case $c_{dd}N^{1/6}=1.5$ (solid line).

Figure 4 shows the real-space Thomas-Fermi surface of the ground state for different trap geometry. The surface of noninteracting fermions has been plotted as dashed lines for comparison. While the shape of the cloud relies on the trap geometry, the dipolar interaction tends to stretch the gas along the dipolar direction also in real space while compressing the gas along the perpendicular radial direction. However, once the trapping potential becomes highly elongated (i.e., $\beta_0\gg 1$), the dipolar interaction tends to shrink the whole cloud in both the radial and the axial directions as shown in the case for $\beta_0=5$ in Fig. 4. This is because, for such a cigar-shaped trap, a number of dipolar fermions align in the axial (dipolar) direction and feel strong mutual attractions. The aspect ratio of the cloud $\sqrt{\langle z^2\rangle_0/\langle x^2\rangle_0}$, normalized to that of noninteracting Fermi gas, for different trap geometry is shown in Fig. 3(b). The deviation of the aspect ratio from the noninteracting case is most dramatic for $\beta_0\approx 1$.

As we have already pointed out, only metastable dipolar gas can exist in a trap. For sufficiently strong dipolar interaction strengths, Eq. (10) no longer supports the local minimum and the system is expected to be unstable against collapse. For a given trap aspect ratio β_0, the onset of this instability gives rise to a critical value for $c_{dd}N^{1/6}$, yielding the phase diagram as shown in Fig. 5. In Ref. [7], Góral *et al.* showed that, for a sufficiently oblate trap, the system is always stable regardless of the strength of the dipolar interaction. The critical trap aspect ratio they found is, when translating to our notation, about $\beta_0\approx 0.33$. As shown by the dashed line in Fig. 5, a result similar to theirs is obtained if we neglect the possibility of Fermi surface deformation by fixing the value of α to 1. The deformation of the Fermi surface, however, changes the phase diagram qualitatively, as represented by the solid line in Fig. 5. The result indicates that no such critical value exists in β_0 — when the trap becomes more and more oblate, the critical dipolar strength

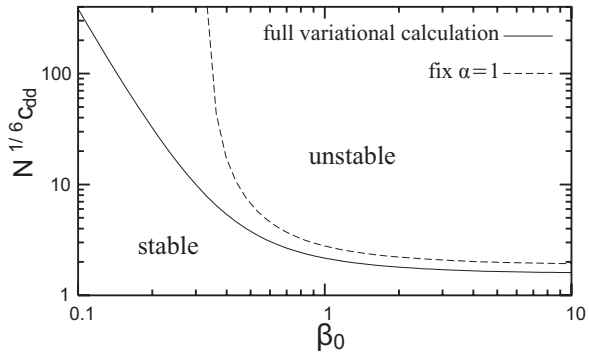

FIG. 5. Critical value of $c_{dd}N^{1/6}$ as a function of β_0. The solid line represents the full variational calculation from our work, while the dashed line is obtained by forcing $\alpha=1$.

increases rapidly but always remains finite. The marked difference between the two curves in Fig. 5 is a clear demonstration of the crucial role played by the Fock exchange term.

Let us now briefly discuss how to detect the dipolar effects in Fermi gases. In fact, the momentum space magnetostriction effect indicates that the dipolar effects will naturally manifest in time-of-flight images. Assuming ballistic expansion after turning off the trapping potential, for time $t \gg 1/\omega$, the aspect ratio of the expanded cloud approaches the initial in-trap aspect ratio of the momentum distribution as shown in Fig. 3(a). In other words, regardless of the initial trap geometry, the expanded cloud will eventually become elongated in the dipolar direction. In comparison, the expansion of a noninteracting Fermi gas is isotropic and results in a spherical cloud in the long-time limit [18,19]. The expansion of a dipolar Fermi gas was recently considered by He *et al.* [20], where they included the effect of the Hartree term (but not the exchange term) during the expansion. The results show that the Hartree term tends to stretch the cloud further in the dipolar direction.

Finally, let us consider how strong the dipolar effect will be for realistic systems. For ^{53}Cr with a magnetic dipole moment of $6\mu_B$, confined in a trap of $\omega=2\pi\times10^2$ Hz and $N=10^6$, we have $c_{dd}N^{1/6}\simeq0.018$, leading to a momentum space aspect ratio about 1.003 for any trap geometry. By contrast, for the same number of polar molecules in the same trap with $m=100$ a.m.u. and a typical electric dipole moment of 1 Debye, we have $c_{dd}N^{1/6}\simeq14.8$ and a corresponding momentum space aspect ratio of 2.81 for $\beta_0=0.2$. This effect will be readily observed in future experiments.

In conclusion, we have analyzed the properties of a dipolar Fermi gas using a variational method that can describe deformation of the phase-space density distribution. We found that the anisotropic nature of the dipolar interaction causes the Fermi surface deformation through the Fock exchange energy. We showed that the Fock exchange term of the dipolar interaction plays a significant role near the critical point and leads to the instability of the dipolar gas for any trap aspect ratio for sufficiently strong dipolar interaction. These effects can be easily observed in polar molecules with large electric dipole moment.

This work is supported by the Grant-in-Aid for the 21st Century COE "Center for Diversity and Universality in Physics" from the Ministry of Education, Culture, Sports, Science and Technology (MEXT) of Japan. H.P. acknowledges support from NSF, the Welch Foundation (Grant No. C-1669), and the W. M. Keck Foundation.

[1] A. Griesmaier, J. Werner, S. Hensler, J. Stuhler, and T. Pfau, Phys. Rev. Lett. **94**, 160401 (2005).
[2] C. A. Stan, M. W. Zwierlein, C. H. Schunck, S. M. F. Raupach, and W. Ketterle, Phys. Rev. Lett. **93**, 143001 (2004); S. Inouye *et al.*, *ibid.* **93**, 183201 (2004); C. Ospelkaus *et al.*, *ibid.* **97**, 120402 (2006); A. J. Kerman, J. M. Sage, S. Sainis, T. Bergeman, and D. Demille, *ibid.* **92**, 033004 (2004); J. M. Sage, S. Sainis, T. Bergemen, and D. Demille, *ibid.* **94**, 203001 (2005); J. Kleinert, C. Haimberger, P. J. Zabawa, and N. P. Bigelow, *ibid.* **99**, 143002 (2007).
[3] M. Baranov *et al.*, Phys. Scr., T **T102**, 74 (2002).
[4] S. Ronen, D. C. E. Bortolotti, and J. L. Bohn, Phys. Rev. A **74**, 013623 (2006); Phys. Rev. Lett. **98**, 030406 (2007).
[5] K. Góral, L. Santos, and M. Lewenstein, Phys. Rev. Lett. **88**, 170406 (2002); S. Yi, T. Li, and C. P. Sun, *ibid.* **98**, 260405 (2007).
[6] S. Yi, L. You, and H. Pu, Phys. Rev. Lett. **93**, 040403 (2004); S. Yi and H. Pu, *ibid.* **97**, 020401 (2006); Y. Kawaguchi, H. Saito, and M. Ueda, *ibid.* **97**, 130404 (2006).
[7] K. Góral, B.-G. Englert, and K. Rzążewski, Phys. Rev. A **63**, 033606 (2001).
[8] K. Góral, M. Brewczyk, and K. Rzążewski, Phys. Rev. A **67**, 025601 (2003).
[9] O. Dutta, M. Jääskeläinen, and P. Meystre, Phys. Rev. A **73**, 043610 (2006).
[10] M. A. Baranov, M. S. Marenko, V. S. Rychkov, and G. V. Shlyapnikov, Phys. Rev. A **66**, 013606 (2002); M. A. Baranov, Ł. Dobrek, and M. Lewenstein, Phys. Rev. Lett. **92**, 250403 (2004).
[11] M. A. Baranov, K. Osterloh, and M. Lewenstein, Phys. Rev. Lett. **94**, 070404 (2005); K. Osterloh, N. Barberán, and M. Lewenstein, *ibid.* **99**, 160403 (2007).
[12] M. Köhl, H. Moritz, T. Stoferle, K. Gunter, and T. Esslinger, Phys. Rev. Lett. **94**, 080403 (2005).
[13] S. Giovanazzi *et al.*, Phys. Rev. A **74**, 013621 (2006).
[14] T. Lahaye *et al.*, Nature (London) **448**, 672 (2007).
[15] P. Ring and P. Schuck, *The Nuclear Many-Body Problem* (Springer-Verlag, Berlin, 1980).
[16] R. J. Dodd *et al.*, Phys. Rev. A **54**, 661 (1996); H. Shi and W. Zheng, *ibid.* **55**, 2930 (1997).
[17] For dipolar BECs at finite temperature, see S. Ronen and J. L. Bohn, Phys. Rev. A **76**, 043607 (2007).
[18] L. Vichi *et al.*, J. Phys. B **31**, L899 (1998).
[19] L. Pitaevskii and S. Stringari, *Bose-Einstein Condensation* (Oxford University Press, Oxford, 2003).
[20] L. He, J. N. Zhang, Y. Zhang, and S. Yi, Phys. Rev. A **77**, 031605(R) (2008).